analytical chemistry

Article

pubs.acs.org/ac

Simultaneous Imaging of Zn^{2+} and Cu^{2+} in Living Cells Based on DNAzyme Modified Gold Nanoparticle

Lu Li, Jie Feng, Yuanyuan Fan, and Bo Tang*

College of Chemistry, Chemical Engineering and Materials Science, Collaborative Innovation Center of Functionalized Probes for Chemical Imaging in Universities of Shandong, Key Laboratory of Molecular and Nano Probes, Ministry of Education, Shandong Provincial Key Laboratory of Clean Production of Fine Chemicals, Shandong Normal University, Jinan 250014, P. R. China

Supporting Information

ABSTRACT: Trace Zn^{2+} and Cu^{2+} in living cells play important roles in the regulation of biological function. It is significant to simultaneously detect the cellular Zn^{2+} and Cu^{2+}. Here, we present a novel two-color fluorescence nanoprobe based on the DNAzymes for simultaneous imaging of Zn^{2+} and Cu^{2+} in living cells. The probe consists of a 13 nm gold nanoparticle, DNAzymes that are specific for Zn^{2+} and Cu^{2+}, and the substrate strands labeled with fluorophores at the 5′ end and quenchers at the 3′ end. The fluorescence of the fluoreophores is quenched both by the gold nanoparticle and the quencher. After the nanoprobes are transferred into the cells, the substrate strands would be cleaved in the presence of the Zn^{2+} and Cu^{2+} target, resulting in disassociation of the shorter DNA fragments containing fluorophores, which produce fluorescence signals correlated with the location and concentration of the Zn^{2+} and Cu^{2+}. The nanoprobe exhibits high specificity, nuclease stability, and good biocompatibility. Moreover, the nanoprobe can simultaneously monitor the cellular Zn^{2+} and Cu^{2+} with an on-site manner, providing the information on localization and concentration of targets, which is significant to further research the Zn^{2+}- and Cu^{2+}-relative cellular events and biological process. The proposed method has shown great potential in the detection of multiple metal ions in living cells, which may help us to better understand the function of metal ions in the fields of biochemistry, molecular biology, and cellular toxicology.

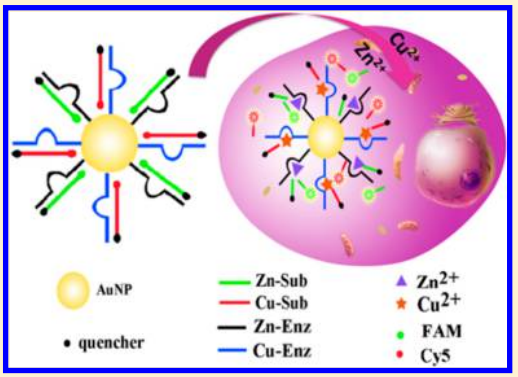

Recently, trace metal ions in the cells are becoming one of the important concerns due to their assignable function in the biological system and deleterious effects on the public health.[1,2] Among these metals, Zn^{2+} is an essential micronutrient element for human life and plays active roles in the gene transcription and neural signal transmission.[3,4] It also constitutes an important component of variety of enzymes and DNA-binding proteins. As another highly chemical reactive metal ion, Cu^{2+} has an important effect on the mitochondrial respiratory chain.[5] Low-level Cu^{2+} is essential for biological activities such as enzyme regulation, metabolism, and immune function.[1,6] However, it has been demonstrated that high-level Cu^{2+} exposure can lead to neural disturbance, liver, or kidney damage,[6−8] as well as serious neurodegenerative diseases and prion diseases.[9−11] Cell signaling pathways are multistage interconnection networks. During the signaling pathways, Zn^{2+} and Cu^{2+}, which have widespread regulation of the biological function, are interactive and complementary to each other. Thus, it is important to simultaneously detect the cellular Zn^{2+} and Cu^{2+} on site. Among the kinds of detection methods for Zn^{2+} and Cu^{2+}, molecular fluorescence imaging is undoubtedly a powerful tool for monitoring the localization and concentration of cellular Zn^{2+} and Cu^{2+} ions. Recently, great progress in the development of various imaging probes based on organic fluorophores and nanomaterials has been made.[12−33] However all of these probes can just detect cellular Zn^{2+} and Cu^{2+} individually. Up to now, the simultaneous on-site imaging of the Zn^{2+} and Cu^{2+} in single cells has not been reported. To meet this requirement, fluorescence probes with high specificity for Zn^{2+} and Cu^{2+} in the complex biological system, consistency in response time for both Zn^{2+} and Cu^{2+}, and resolvability in fluorescence spectra of Zn^{2+} and Cu^{2+} for imaging should be developed.

DNAzymes, which are isolated through in vitro selection, have been regarded as novel and ideal platforms in sensing due to their catalytic ability and binding activity toward specific metal ions.[34−38] As a result of the complicated selection process, the obtained DNAzymes exhibit high specificity toward the targets. Moreover, comparing with organic fluorophores and genetically encoded protein sensors, it does not need expert knowledge to design a metal-binding site, it is also easy to synthesize, modify, and assemble the DNAzymes. Recently, it has been utilized in the detection of metal ions in solution.[39−49] Furthermore, the DNAzymes are biocompatible, naturally water-soluble, and have low toxicity.[38,50−53] These advantages make the DNAzymes very suitable for the monitoring of metal ions in the intracellular environment.

Received: January 16, 2015
Accepted: April 8, 2015
Published: April 8, 2015

DOI: 10.1021/acs.analchem.5b00204
Anal. Chem. 2015, 87, 4829−4835

However, up to now, when DNAzymes were used, only uranyl ion in living cells was imaged.[54]

To realize the simultaneous imaging of the Zn^{2+} and Cu^{2+} in living cells, we present a two-color fluorescence nanoprobe based on the DNAzyme-modified gold nanoparticle (AuNP). To construct the nanoprobe, a 13 nm AuNP, which is chosen as cellular carrier and fluorescence quencher, is assembled with Zn^{2+}-specific DNAzyme (Zn-Enz) and Cu^{2+}-specific DNAzyme (Cu-Enz) by gold−thiol bond.[55−57] Two substrate strands named Zn-Sub and Cu-Sub are hybridized with the Zn-Enz and Cu-Enz, respectively. The substrate strands are labeled with fluorophores at the 5′ end (FAM on Zn-Sub and Cy5 on Cu-Sub) and quenchers at the 3′ end (BHQ-1 on Zn-Sub and BHQ-2 on Cu-Sub). The fluorescence of the two fluorophores is quenched both by the gold nanoparticle and the quencher. After the nanoprobe is transferred into cells, in the presence of the Zn^{2+} and Cu^{2+} target, the substrate strands are cleaved, resulting in the disassociation of the shorter DNA fragments containing fluorophores, which would produce fluorescence signals correlated with the location and concentration of the cellular Zn^{2+} and Cu^{2+} target. The details of this nanoprobe are shown as Scheme 1. The nanoprobe takes advantages of the unique properties of gold nanoparticle, including great quenching efficiency,[58] stability in biosystem,[59] ability to enter cells without use of transfection agents,[60] resistance to degradation,[61] and much larger DNA loading efficiency than conventional transfection methods, which is beneficial for detection of multiple targets.[62] Moreover, the nanoprobe can simultaneous monitor the cellular Zn^{2+} and Cu^{2+} with an on-site manner, providing the information on localization and concentration of targets. It is significant to further understand the Zn^{2+}- and Cu^{2+}-relative cellular events and biological process. The proposed strategy would have potential application in the detection of multiple metal ions in living cells, helping us better understanding the function of metal ions in the fields of biochemistry, molecular biology, and cellular toxicology.

Scheme 1. Scheme of the Simultaneous Imaging of Zn^{2+} and Cu^{2+} in Living Cells Based on DNAzyme-Modified AuNP

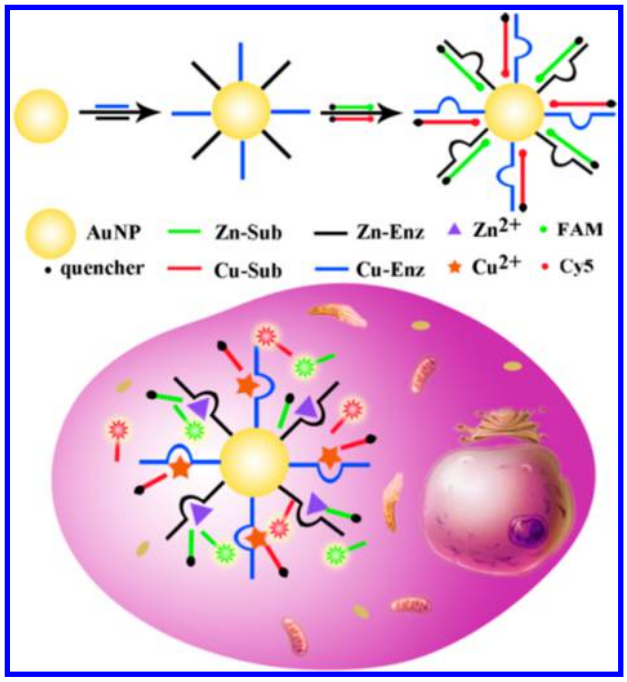

EXPERIMENTAL SECTION

Materials and Reagents. Oligonucleotides Zn-Enz (5′-CATCTCTTCTCCGAGCCGGTCGAAATAGTGAGT$(A)_9(CH_2)_6$SH-3′), Zn-Sub (5′-FAM-ACTCACTAT**rA**GG-AAGAGATG-BHQ-1−3′ or 5′-FAM-ACTCACTAT**rA**G-GAAGAGATG-3′), Cu-Enz (5′-GGTAAGCCTGG-GCCTCTTTCTTTTTAAGAAAGAAC$(A)_9(CH_2)_6$SH-3′), and Cu-Sub (5′- Cy5-AGCTTCTTTC-TAATACG**G**CTTACC-BHQ-2−3′ or 5′- Cy5-AGCTTCTT-TCTAATACG**G**CTTACC-3′), inert-Enz (5′- Cy3-AGTTGTATACATTGTGAATAGCTCCATGTCCTA$(A)_9(CH_2)_6$SH-3′ or (5′-AGTTGTATAC-ATTGTGAATAGCTCCATGTCCTA $(A)_9(CH_2)_6$SH-3′), inert-Sub (5′-TAGGACATGAGTATACAACT-3′) were synthesized by Sangon Biotech Co., Ltd. (Shanghai, China) and purified by high-performance liquid chromatography (HPLC). 3-(4,5-Dimethyl-thiazol-2-yl)-2,5-diphenyltetrazolium bromide (MTT) were purchased from Sigma Chemical Company. Hydrogen tetrachloroaurate (III) ($HAuCl_4{\cdot}4H_2O$, 99.99%), Trisodium citrate ($C_6H_5Na_3O_7{\cdot}2H_2O$), Sodium dodecyl sulfate (SDS), KCl, NaCl, $Cu(CH_3COO)_2{\cdot}H_2O$, $Mn(CH_3COO)_2{\cdot}4H_2O$, $Co(CH_3COO)_2{\cdot}4H_2O$, $Cd(NO_3)_2{\cdot}6H_2O$, $Zn(CH_3COO)_2{\cdot}2H_2O$, $CaCl_2$, $FeCl_3$ and $Ni(CH_3COO)_2{\cdot}4H_2O$ were purchased from China National Pharmaceutical Group Corporation (Shanghai, China). Cell culture products, unless mentioned otherwise, were purchased from GIBCO. The human liver cancer cell line HepG2 was purchased from KeyGEN biotechnology Company (Nanjing, China). All the chemicals were of analytical grade and used without further purification. Deionized water was obtained through a Sartorius Arium 611 VF system (Sartorius AG, Germany) to a resistivity of 18.2 MΩ·cm.

Instrumentation. Transmission electron microscopy (TEM) was carried out on a JEOL JEM 2010 electron microscope. All pH measurements were performed with a pH-3c digital pH-meter (Shanghai LeiCi Device Works, Shanghai, China) with a combined glass-calomel electrode. Centrifugation was performed with a Sigma 3K15 refrigerated centrifuge. UV−vis spectra were recorded from a Hitachi U-3010 UV−vis spectrometer. The fluorescent spectra were measured using Cary Eclipse fluorescence spectrophotometer (Varian, California). Absorbance was measured in a microplate reader (RT 6000, Rayto, U.S.A.) in the MTT assay. Confocal fluorescence imaging studies were performed with a TCS SP5 confocal laser scanning microscopy (Leica Co., Ltd. Germany) with an objective lens (40×).

Preparation of AuNPs. The 13 nm AuNPs were prepared by the classical citrate reduction route.[63] All the glassware was first cleaned with a mixture of HCl and HNO_3 (ratio of HCl/HNO_3 = 3:1 in volume) and thoroughly rinsed with ultrapure water. Then 100 mL of 0.01% aqueous chlorauric acid solution was brought to a boil, and 3.5 mL of 1% sodium citrate solution was added quickly, which resulted in a change in solution color from pale yellow to deep red. The solution was further boiled for 15 min and then left to cool to room temperature while stirring. Transmission electron microscopy (TEM) images indicated the particle sizes are ∼13 nm. The prepared AuNPs were stored at 4 °C.

Preparation of Enzs-Modified AuNPs. AuNPs were modified with Enzs (Zn-Enz and Cu-Enz) according to

DOI: 10.1021/acs.analchem.5b00204
Anal. Chem. 2015, 87, 4829−4835

published protocols with slight modifications.[62,64] Briefly, two Enzs (Zn-Enz and Cu-Enz) were mixed and added to a solution of Au NPs (3 nM) with a final concentration of 0.4 μM each and shaken overnight. After 16 h, SDS solution (10%) was added to the mixture to achieve 0.1% SDS concentration. Then phosphate (NaH_2PO_4/Na_2HPO_4) buffer (0.1 M, pH 7.4) was added to the mixture to achieve 0.01 M phosphate concentration. In the subsequent salt aging process, the mixture solution was first brought to 0.05 M of NaCl by dropwise addition of 2 M NaCl solution and allowed to stand for 6 h. The mixture was next salted to 0.1 M for 6 h, salted to 0.2 M for further incubation for 6 h, and lastly, salted to 0.3 M NaCl. The solution was centrifuged (13 500*g*, 20 min) and resuspended in 0.01 M phosphate buffer saline (0.3 M NaCl, pH 7.4) for three times. Then the nanoprobe were resuspended in 0.01 M PBS and stored in the dark at 4 °C. The concentration of Au NPs was determined by measuring their extinction at 518 nm ($\varepsilon = 2.7 \times 10^8$ L mol^{-1} cm^{-1}).

Quantitation of Enzs Loaded on the AuNPs. The three stands (FAM-labeled Zn-Enz stands, Cy5-labeled Cu-Enz stands, Cy3-labeled inert stands) loaded on AuNPs were quantitated according to the previous protocol.[65] Briefly, mercaptoethanol was added (final concentration 20 mM) to the probe solution (3 nM). After it was incubated overnight with shaking at room temperature, the fluorochrome-labeled stands were released. Then the fluorochrome-labeled stands were collected via centrifugation and the fluorescence was measured with a fluorescence spectrometer. The fluorescence of FAM was collected between 500 and 600 nm by use of the maximal excitation wavelength at 488 nm; the fluorescence of Cy3 was collected between 555 and 655 nm by use of the maximal excitation wavelength at 550 nm; and the fluorescence of Cy5 was collected between 650 and 750 nm by use of the maximal excitation wavelength at 635 nm. The fluorescence was converted to molar concentrations of fluorochrome using a standard linear calibration curve that was prepared with known concentrations of fluorochrome-labeled stands with identical buffer pH, ionic strength, and ME concentrations.

Hybridization Experiment. The Subs (Zn-Sub and Cu-Sub, 10 μM) were added to 200 μL of 10 nM Enzs-AuNP (Zn-Enz-AuNP and Cu-Enz-AuNP) solution. The mixture was heated at 43 °C for 3 h. Then the mixture was centrifuged (13 500*g*, 20 min) and resuspended in 0.01 M PBS in order to remove excess Subs. Finally, the nanoprobe was dispersed in 200 μL of 0.01 M PBS for further use.

Fluorescence Measurements. A certain concentration of Zn^{2+} and Cu^{2+} stock solution was added into the nanoprobe solution. After reaction at 37 °C for 30 min, the fluorescence of FAM was collected between 500 and 600 nm by use of the maximal excitation wavelength at 488 nm, and the fluorescence of Cy5 was collected between 650 and 750 nm by use of the maximal excitation wavelength at 635 nm.

Selectivity Experiment. The Zn^{2+} and Cu^{2+} stock solutions were added into the nanoprobe solution with a final concentration of 100 nM. For the other metal ions, the concentrations were the following: 1.0 mM for K^+ and Ca^{2+}; 25 μM for Fe^{3+}; Co^{2+}, Ni^{2+}, Mn^{2+}, Cd^{2+}, Pb^{2+}; and 50 μM for PDCA. The measuring processing was the same as above.

Nuclease Assay. Two groups of the nanoprobe were placed in a 96-well fluorescence microplate at 37 °C. After allowing the samples to equilibrate (10 min), 1.3 μL of DNase I in assay buffer (2 U/L) was added to one group. The fluorescence of these samples was monitored for 1 h. Then 100 nM DNA targets were added in parallel into the two samples with incubation for 30 min at 37 °C. The fluorescence was measured at appropriate excitation wavelengths after the solution was cooled to room temperature.

Cell Culture. HepG2 cells were cultured in DMEM supplemented with 10% fetal bovine serum, 100 U/mL penicillin, and 100 μg/mL streptomycin and incubated at 37 °C in a humidified atmosphere of 5% CO_2 and 95% air.

Cellular Uptake of the Zn^{2+} and Cu^{2+}. To determine the cellular concentration of Zn^{2+} and Cu^{2+}, one group of cells was washed with PBS three times after incubation with the Zn^{2+} and Cu^{2+} (5 μM) for 60 min. Then the cells were trypsinized to remove them from the bottom and collected in centrifuge tubes. Next, the cells were treated with 0.2 mL of aqua regia (3:1 hydrochloric acid/nitric acid). Following the incubation overnight, the sample was diluted to 10 mL using ultrapure water. The sample was then analyzed for total zinc or copper content by ICP-AES. As control, another group of cells without regulation was served. Other steps were performed as described above. The concentrations of cellular free Zn^{2+} and Cu^{2+} were estimated by subtracting the concentration of zinc and copper in the control group cells from the concentration of zinc and copper in the experimental group cells. It was estimated that the cellular concentration of Zn^{2+} and Cu^{2+} were ~1.8 μM and ~625 nM, respectively.

Cellular Uptake of the AuNPs. To estimate the amount of AuNP per cell, cells were washed with PBS three times after incubation with the nanoprobe (5 nM) for 3 h. Then the cells were trypsinized to remove them from the bottom and collected in centrifuge tubes. Next, the cells were treated with 0.2 mL of aqua regia (3:1 hydrochloric acid/nitric acid). Following the incubation overnight, the sample was diluted to 10 mL using ultrapure water. The sample was then analyzed for total gold content by ICP-AES. Based on the previous protocol,[66,67] the number of Au NPs in each cell was calculated to be 9×10^5.

MTT Assay. To investigate the cytotoxicity of the nanoprobe, a MTT assay was carried out when the nanoprobe existed. HepG2 cells (1×10^6 cells/well) were dispersed within replicate 96-well microtiter plates to a total volume of 200 μL well^{-1}. Plates were maintained at 37 °C in a 5% CO_2/95% air incubator for 24 h. After the original medium was removed, HepG2 cells were incubated with unmodified Au NPs (1 nM), nanoprobe (1 nM and 5 nM) for 6, 12, 24, and 48 h. Then, 100 μL of MTT solution (0.5 mg mL^{-1} in PBS) was added to each well. After 4 h, the remaining MTT solution was removed, and 150 μL of DMSO was added to each well to dissolve the formazan crystals. The absorbance was measured at 490 nm with a RT 6000 microplate reader.

Imaging Intracellular Zn^{2+} and Cu^{2+}. First, HepG2 cells were cultured in DMEM for 24 h. Next, the cells were incubated with 5 μM Zn^{2+} and 5 μM Cu^{2+} at 37 °C in 5% CO_2 for 60 min, and then the cells were washed three times with fresh DMEM. Finally, the nanoprobe (5 nM) was delivered into HepG2 cells in DMEM culture medium for 3 h, and then the cells were washed three times with PBS. Fluorescence images were acquired on a confocal laser scanning microscope with different laser transmitters. The Zn^{2+} was recorded by FAM in green channel with 488 nm excitation, Cu^{2+} was recorded by Cy5 in red channel with 633 nm excitation. HepG2 cells incubated with 5 μM Cu^{2+}, 5 μM Zn^{2+} or without metal ions, respectively, were served as control. Other steps were performed as described above.

DOI: 10.1021/acs.analchem.5b00204
Anal. Chem. 2015, 87, 4829−4835

RESULTS AND DISCUSSION

It has been reported that 13 nm AuNP are efficient quenchers,[58] can be densely functionalized with DNA,[68−70] and do not efficiently scatter visible light,[60] which is important for designing optical probes with minimal interference.[70] Thus, we chose the 13 nm AuNP as carrier to construct the nanoprobe. The enzyme strands were immobilized onto the AuNP by gold−thiol bond. In addition, a poly-A spacer was added between the thiol moiety and the enzyme strands for extending the enzyme strands to hybridize completely with the substrate strands and avoid loss of activity due to steric interference of the AuNP.[54] The substrate strands were hybridized with enzyme strands by heating and annealing. As signal reporter, fluorophores FAM and Cy5 were labeled at the 5′ end of the substrate strands, respectively. BHQ-1 and BHQ-2 as quencher were also labeled at the 3′ end of the substrate strands, respectively. Fluorescence from FAM and Cy5 could be mostly quenched both by the AuNP and the quencher as a result of the nanometal surface energy transfer (NSET) and fluorescence resonance energy transfer (FRET), respectively.[71] Compared with the fluorescence from only AuNP quenching (purple curve), the obviously decreased fluorescent background accompanied by the AuNP and the quencher labeling (red curve) illustrated higher S/N ratio could be obtained by the design of the double-quencher labeling.[54] In the presence of Zn^{2+} and Cu^{2+}, the substrates were irreversibly cleaved at the cleavage site, causing the release of the shorter DNA fragment and recovery of the fluorescence signal that is correlated with the location and concentration of the Cu^{2+} and Zn^{2+} target.

The TEM image of AuNPs (Supporting Information, Figure S1) indicated an average size of 13 nm and verified the formation of spherical AuNPs. The UV−vis absorption spectra indicated that the maximum absorption of the AuNP was at 519 nm and that it was red-shifted to 524 nm for the nanoprobe, which confirmed that the AuNPs were successfully functionalized with enzyme strands (Supporting Information, Figure S2). Quantification of the enzyme strands on the AuNP surface based on the previously established method,[65] showed that each AuNP carried 30 ± 2 Zn-Enz stands and 22 ± 2 Cu-Enz stands (Supporting Information, Figure S3), and the same number of substrate strands hybridized to the enzyme strands. To demonstrate the feasibility of our design, fluorescence spectra of a solution (0.01 M PBS, 0.3 M NaCl, pH = 7.4) are recorded. After the solution was excited by a 488 nm laser, the fluorescence signal correlated with Zn^{2+} could be observed. As shown in Figure 1a, the fluorescence of the AuNP and the enzyme strands modified AuNP are negligible (green and blue curve). After the substrate strands were hybridized with the enzyme strands, faint fluorescence was observed due to the incomplete quenching of FAM (red curve). Upon the addition of Zn^{2+} (20 nM), the fluorescence intensity at 524 nm increased more than 4-fold (black curve). Using the same probe, fluorescence at 665 nm could also be observed with the exciting at 635 nm after Cu^{2+} was added into the solution (Figure 1b). These results illustrate that the nanoprobe is an effective turn-on fluorescence nanoprobe and has the ability to simultaneously detect the Zn^{2+} and Cu^{2+} as a result of its good resolvability in fluorescence spectra of Zn^{2+} and Cu^{2+}.

The sensitivity, selectivity, and response time of the nanoprobe were then investigated. Figure 2 shows that the fluorescence intensity of the nanoprobe increases with increasing concentration of the Zn^{2+} and Cu^{2+} from 0 to 5

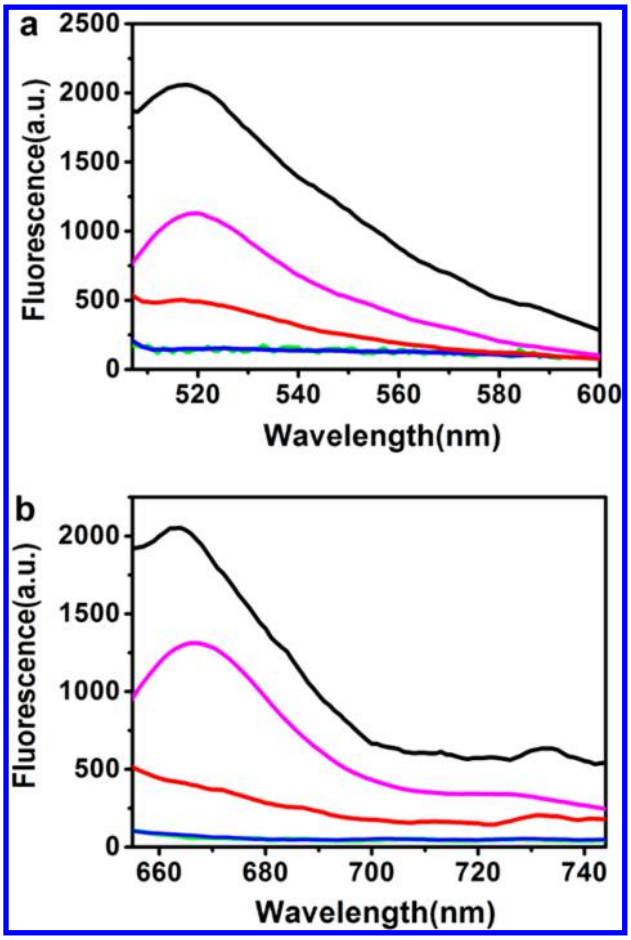

Figure 1. Fluorescence spectra of the AuNP (green curve), the Enz-AuNP (blue curve), the AuNP-Enz-Sub-FAM , or AuNP-Enz-Sub-Cy5 (purple curve); the nanoprobe with double-quencher labeling in the absence (red curve) and presence (black curve) of Zn^{2+} and Cu^{2+} ions. The concentrations of Zn^{2+} and Cu^{2+} were 20 nM, respectively. (a) The curve for Zn^{2+} measured with 488 nm excitation; (b) the curve for Cu^{2+} measured with 635 nm excitation.

μM, respectively. The fluorescence spectra associated with the concentration of the metal ions targets. But the result was influenced by the relative density changes of Zn-Enz stands and Cu-Enz stands loaded on AuNP (Supporting Information, Figure S4). A good linearity was obtained from 1 nM to 30 nM of Zn^{2+} and 1 nM to 20 nM of Cu^{2+}. The detection limit of the nanoprobe was calculated to be 0.47 nM for Zn^{2+} and 0.45 nM for Cu^{2+} on the basis of the 3σ/slope. Furthermore, the fluorescent responses from a mixed sample with both zinc and copper have been investigated. The sum of responses from separate samples with zinc and copper were almost the same with the net response from a mixed sample with both zinc and copper (Supporting Information, Figure S5). To evaluate the selectivity of the nanoprobe for sensing Zn^{2+} and Cu^{2+}, other various biologically relevant metal ions, including Mn^{2+}, Cd^{2+}, Mg^{2+}, Co^{2+}, Fe^{3+}, Ca^{2+}, K^{+}, and Ni^{2+}, were evaluated. The interference of Pb^{2+} can be eliminated by the addition of 2,6-pyridinedicarboxylic acid (PDCA), that act as a selective ligand for binding Pb^{2+} ions.[72] As shown in Figure 3, the nanoprobe exhibited 3- to 4-fold higher fluorescence signal for Zn^{2+} and Cu^{2+}, as compared to other metal ions with higher concentration. The excellent selectivity makes the nanoprobe suitable for working in the complex biological system. A

DOI: 10.1021/acs.analchem.5b00204
Anal. Chem. 2015, 87, 4829−4835

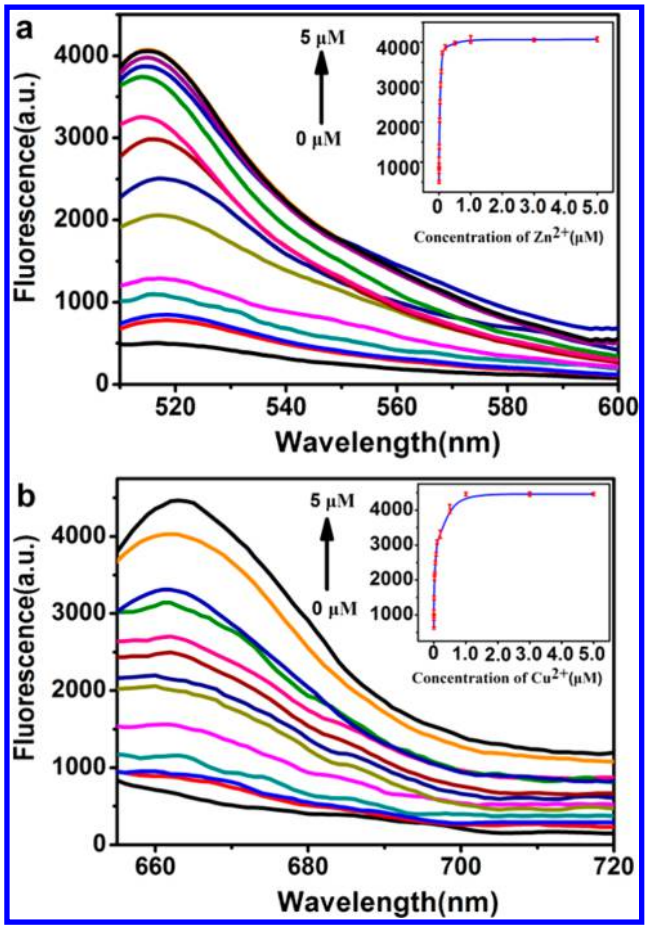

Figure 2. Fluorescence spectra of the nanoprobe in the presence of various concentrations of Zn^{2+} and Cu^{2+} (0, 1, 2, 5, 10, 20, 30, 50, 75, 100, 200, 500, 1000, 3000, and 5000 nM) measured with different excitation wavelength, respectively. Inset: calibration curves for the fluorescence intensity versus corresponding target concentrations. (a) The curve for Zn^{2+} measured with 488 nm excitation; (b) the curve for Cu^{2+} measured with 635 nm excitation. Error bars were estimated from three replicate measurements.

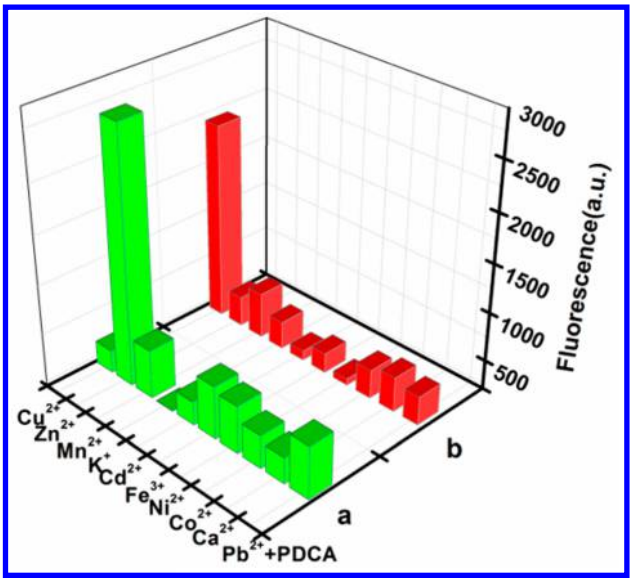

Figure 3. Specificity of the nanoprobe over several metal ions. The nanoprobe was mixed with Zn^{2+} (100 nM), Cu^{2+} (100 nM) and other metal ions (1.0 mM of Ca^{2+} and K^{+}; 25 μM of Mn^{2+}, Co^{2+}, Fe^{3+}, Ni^{2+}, Cd^{2+}; and 25 μM of Pb^{2+} with 50 μM for PDCA) measured with 488 nm excitation wavelength (a) and 635 nm excitation wavelength (b).

kinetics study was also carried out to record the time-dependent fluorescence intensity changes at 524 nm and 665 nm after the addition of 20 nM of Zn^{2+} and Cu^{2+}. As shown in Figure S6, the fluorescence intensity both from the Zn^{2+} and Cu^{2+} gradually increased with the reaction time and then reached plateaus after 30 min. The consistency of the nanoprobe in response time for the both metal ions ensures simultaneous imaging will be realized.

Nuclease stability and cytotoxicity are key properties of probes for applications in living cells. A fluorescence test was conducted to evaluate the stability of the nanoprobe, using the enzyme deoxyribonuclease I (DNaseI).[61] The results showed that there was no obvious increase of fluorescence signal observed after the nanoprobe was treated with DNaseI compared to the probe without DNaseI (Supporting Information, Figure S7), suggesting no cleavage of substrate strands. This indicates that the nanoprobe possesses high resistance to nuclease. To evaluate the cytotoxicity of the nanoprobe, we performed an MTT (3-(4,5-dimethylthiazol-2-yl)-2,5-diphe- nyltetrazolium bromide) assay in human liver cer cell line HepG2. The absorbance of MTT at 490 nm is dependent upon the degree of activation of the cells. The cell viability is then expressed by the ratio of the absorbance of the cells incubated with the nanoprobe to that of the cells incubated with the culture medium only. The results indicated that the nanoprobe (1 nM and 5 nM) showed almost no cytotoxicity or side effects in living cells (Supporting Information, Figure S8). These results confirm that the nanoparticle has low toxicity and its stability is sufficient for application in cellular environments. We next tested the application of the nanoprobe in living cells. Cellular uptake and fluorescence response of the nanoprobe for cellular Zn^{2+} and Cu^{2+} were performed using HepG2 cells as a model. HepG2 cells were first treated with 5 μM Zn^{2+} and 5 μM Cu^{2+} for 1 h to allow sufficient metal ions uptake. Based on ICP-AES, the intracellular free concentration of Zn^{2+} and Cu^{2+} under these conditions are estimated to reach 1.8 μM and 625 nM, respectively. Then, the HepG2 cells were incubated with the probes for another 3 h before images were taken using confocal laser scanning microscopy (CLSM). According to the studies in the literature,[54,73] the AuNP-DNAzymes nanoprobe could enter the cells via receptor-mediated endocytosis and mostly located in lysosomes. The uptake of the nanoprobe in HepG2 cells was also confirmed by the ICP-AES. As shown in Figure 4, a strong green fluorescence signal corresponding to Zn^{2+} and a red fluorescence signal corresponding to Cu^{2+} were observed. As a control, HepG2 cells treated with 5 μM Zn^{2+} or 5 μM Cu^{2+} or no metal ions were also incubated with the nanoprobe and imaged under the same conditions. Obvious green fluorescence was observed from the cells treated with Zn^{2+}. Similarly, obvious red fluorescence was observed from cells treated with Cu^{2+} and faint fluorescence signal was produced in the cells without pretreatment using metal ions. The result indicates that the nanoprobe can be used as a fluorescence probe for the simultaneous detection of Zn^{2+} and Cu^{2+} in single cells. Bright-field images confirmed that the cells were viable throughout the imaging experiments.

DOI: 10.1021/acs.analchem.5b00204
Anal. Chem. 2015, 87, 4829−4835

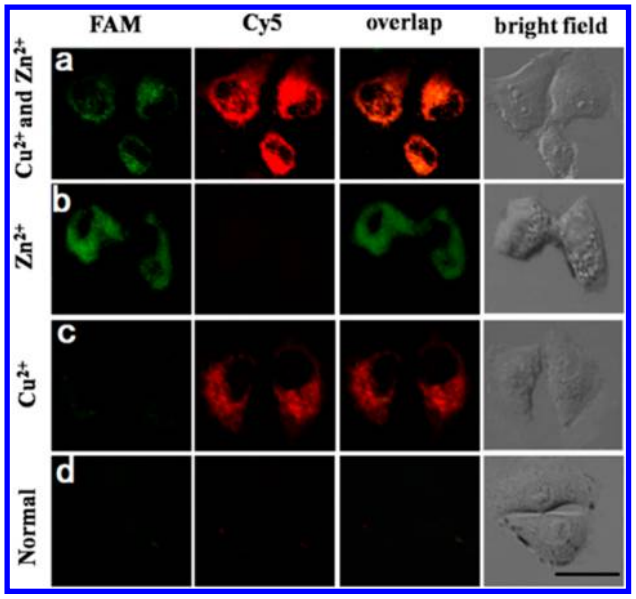

Figure 4. Intracellular imaging of Zn^{2+} and Cu^{2+} under CLSM. Confocal microscopy images of HepG2 cells treated with Zn^{2+} and Cu^{2+} (a), only Zn^{2+} (b), only Cu^{2+} (c), and no metal ions (d). The Zn^{2+} was recorded using FAM in the green channel with excitation at 488 nm; the Cu^{2+} was recorded using Cy5 in the red channel with excitation at 633 nm. Scale bar is 25 μm.

CONCLUSIONS

In summary, we designed and assembled a two-color fluorescence nanoprobe based on the DNAzymes modified AuNP and realized the simultaneous on-site imaging of the Zn^{2+} and Cu^{2+} in living cells. The nanoprobe exhibited high specificity, nuclease stability, and good biocompatibility. The results of the simultaneous detection of the Zn^{2+} and Cu^{2+} provided the information on localization and concentration of targets, which would be beneficial in further understanding the Zn^{2+} and Cu^{2+} relative cellular events and biological process. The proposed strategy would have potential application in the detection and imaging of multiple metal ions in living cells.

ASSOCIATED CONTENT

Supporting Information

Description of supplementary figures S1–S8. This material is available free of charge via the Internet at http://pubs.acs.org.

AUTHOR INFORMATION

Corresponding Author

*E-mail: tangb@sdnu.edu.cn.

Notes

The authors declare no competing financial interest.

ACKNOWLEDGMENTS

This work was supported by 973 Program (2013CB933800), National Natural Science Foundation of China (21227005, 21390411, 91313302 and 21205074), and the Specialized Research Fund for the Doctoral Program of Higher Education of China (Grants 20123704120006).

REFERENCES

(1) Liu, M.; Zhao, H.; Chen, S.; Yu, H.; Zhang, Y.; Quan, X. *Biosens. Bioelectron* **2011**, *26*, 4111–4116.
(2) Zhang, L.; Zhang, Y. M.; Liang, R. P.; Qiu, J. D. *J. Phys. Chem. C* **2013**, *117*, 12352–12357.
(3) Nies, D. H. *Appl. Microbiol. Biotechnol.* **1999**, *51*, 730–750.
(4) Carol, P.; Sreejith, S.; Ajayaghosh, A. A. *Chem.—Asian J.* **2007**, *2*, 338–348.
(5) Şengör, S. S.; Gikas, P.; Moberly, J. G.; Peyton, B. M.; Ginn, T. R. *J. Chem. Technol. Biotechnol.* **2012**, *87*, 374–380.
(6) Balch, P. A. *Prescription for Nutritional Healing*, 4th ed.; Penguin Press: New York, 2006; p 431, 534.
(7) Georgopoulos, P. G.; Roy, A.; Yonone-Lioy, M. J.; Opiekun, R. E.; Lioy, P. J. *J. Toxicol. Environ. Health, Part B* **2001**, *4*, 341–394.
(8) Zietz, B. P.; Dieter, H. H.; Lakomek, M.; Schneider, H.; Kebler-Gaedtke, B.; Dunkelberg, H. *Sci. Total Environ.* **2003**, *302*, 127–144.
(9) Brown, D. R.; Kozlowski, H. *Dalton Trans.* **2004**, 1907–1917.
(10) Vulpe, C.; Levinson, B.; Whitney, S.; Packman, S.; Gitschier, J. *Nat. Genet.* **1993**, *3*, 7–13.
(11) Waggoner, D. J.; Bartnikas, T. B.; Gitlin, J. D. *Neurobiol. Dis.* **1999**, *6*, 221–230.
(12) Anbu, S.; Ravishankaran, R.; Silva, M. F. C. G.; Karande, A. A.; Pombeiro, A. J. L. *Inorg. Chem.* **2014**, *53*, 6655–6664.
(13) Meng, Q. T.; Zhang, X. L.; He, C.; He, G. J.; Zhou, P.; Duan, C. Y. *Adv. Funct. Mater.* **2010**, *20*, 1903–1909.
(14) Zhu, A. W.; Qu, Q.; Shao, X. L.; Kong, B.; Tian, Y. *Angew. Chem., Int. Ed.* **2012**, *51*, 7185–7189.
(15) Li, P.; Duan, X.; Chen, Z.; Liu, Y.; Xie, T.; Fang, L.; Li, X.; Yin, M.; Tang, B. *Chem. Commun.* **2011**, *47*, 7755–7757.
(16) Huang, L.; Wang, X.; Xie, G.; Xi, P.; Li, Z.; Xu, M.; Wu, Y.; Bai, D.; Zeng, Z. *Dalton Trans.* **2010**, *39*, 7894–7846.
(17) Kim, H. M.; Seo, M. S.; An, M. J.; Hong, J. H.; Tian, Y. S.; Choi, J. H.; Kwon, O.; Lee, K. J.; Cho, B. R. *Angew. Chem., Int. Ed.* **2008**, *47*, 5167–5170.
(18) Li, Z.; Yu, M.; Zhang, L.; Yu, M.; Liu, J.; Wei, L.; Zhang, H. *Chem. Commun.* **2010**, *46*, 7169–7171.
(19) Tang, B.; Huang, H.; Xu, K.; Tong, L.; Yang, G.; Liu, X.; An, L. *Chem. Commun.* **2006**, 3609–3611.
(20) John, C. L.; Huan, Y.; Wu, X.; Jin, Y.; Pierce, D. T.; Zhao, J. X. *Analyst* **2013**, *138*, 4950–4957.
(21) Xue, L.; Li, G.; Zhu, D.; Liu, Q.; Jiang, H. *Inorg. Chem.* **2012**, *51*, 10842–10849.
(22) Xue, L.; Liu, C.; Jiang, H. *Chem. Commun.* **2009**, 1061–1063.
(23) Simmons, J. T.; Allen, J. R.; Morris, D. R.; Clark, R. J.; Levenson, C. W.; Davidson, M. W.; Zhu, L. *Inorg. Chem.* **2013**, *52*, 5838–5850.
(24) Liu, Z.; Zhang, C.; Chen, Y.; Qian, F.; Bai, Y.; He, W.; Guo, Z. *Chem. Commun.* **2014**, *50*, 1253–1255.
(25) Zhang, C.; Liu, Z.; Li, Y.; He, W.; Gao, X.; Guo, Z. *Chem. Commun.* **2013**, *49*, 11430–11432.
(26) Du, P.; Lippard, S. J. *Inorg. Chem.* **2010**, *49*, 10753–10755.
(27) Chen, H.; Gao, W.; Zhu, M.; Gao, H.; Xue, J.; Li, Y. *Chem. Commun.* **2010**, *46*, 8389–8391.
(28) Carter, K. P.; Young, A. M.; Palmer, A. E. *Chem. Rev.* **2014**, *114*, 4564–4601.
(29) Meng, X.; Wang, S.; Li, Y.; Zhu, M.; Guo, Q. *Chem. Commun.* **2012**, *48*, 4196–4198.
(30) Liu, Z.; Zhang, C.; Chen, Y.; He, W.; Guo, Z. *Chem. Commun.* **2012**, *48*, 8365–8367.
(31) Lin, W.; Long, L.; Chen, B.; Tan, W.; Gao, W. *Chem. Commun.* **2010**, *46*, 1311–1313.
(32) Yu, F. B.; Zhang, W. S.; Li, P.; Xing, Y. L.; Tong, L.; Ma, J. P.; Tang, B. *Analyst* **2009**, *134*, 1826–1833.
(33) Tang, B.; Niu, J. Y.; Yu, C. G.; Zhuo, L. H.; C, G. J. *Chem. Commun.* **2005**, *33*, 4184–4186.
(34) Breaker, R. R. *Science* **2000**, *290*, 2095–2096.
(35) Ellington, A. D.; Szostak, J. W. *Nature* **1990**, *346*, 818–822.
(36) Tuerk, C.; Gold, L. *Science* **1990**, *249*, 505–510.
(37) Famulok, M.; Hartig, J. S.; Mayer, G. *Chem. Rev.* **2007**, *107*, 3715–3743.
(38) Breaker, R. R.; Joyce, G. F. *Chem. Biol.* **1994**, *1*, 223–229.

DOI: 10.1021/acs.analchem.5b00204
Anal. Chem. 2015, 87, 4829–4835

(39) Zhao, X. H.; Kong, R. M.; Zhang, X. B.; Meng, H. M.; Liu, W. N.; Tan, W. H.; Shen, G. L.; Yu, R. Q. *Anal. Chem.* **2011**, *83*, 5062−5066.
(40) Yu, Y.; Liu, Y.; Zhen, S. J.; Huang, C. Z. *Chem. Commun.* **2013**, *49*, 1942−1944.
(41) Wang, H. B.; Wang, L.; Huang, K. J.; Xu, S. P.; Wang, H. Q.; Wang, L. L.; Liu, Y. M. *New J. Chem.* **2013**, *37*, 2557−2563.
(42) Liu, J. W.; Lu, Y. *J. Am. Chem. Soc.* **2007**, *131*, 9838−9839.
(43) Yin, B. C.; Ye, B. C.; Tan, W. H.; Wang, H.; Xie, C. C. *J. Am. Chem. Soc.* **2009**, *131*, 14624−14625.
(44) Wu, C. S.; Oo, M. K. K.; Fan, X. D. *ACS Nano* **2010**, *4*, 5897−5904.
(45) Li, J.; Zheng, W. C.; Kwon, A. H.; Lu, Y. *Nucleic Acids Res.* **2000**, *28*, 481−488.
(46) Lan, T.; Furuya, K.; Lu, Y. *Chem. Commun.* **2010**, *46*, 3896−3898.
(47) Liu, M.; Zhao, H.; Chen, S.; Yu, H.; Zhang, Y.; Quan, X. *Chem. Commun.* **2011**, *47*, 7749−7751.
(48) Nie, D.; Wu, H.; Zheng, Q.; Guo, L.; Ye, P.; Hao, Y.; Li, Y.; Fu, F.; Guo, Y. *Chem. Commun.* **2012**, *48*, 1150−1152.
(49) Liu, J. W.; Cao, Z. H.; Lu, Y. *Chem. Rev.* **2009**, *109*, 1948−1998.
(50) Mei, S. H. J.; Liu, Z.; Brennan, J. D.; Li, Y. F. *J. Am. Chem. Soc.* **2003**, *125*, 412−420.
(51) Breaker, R. R.; Joyce, G. F. *Chem. Biol.* **1994**, *1*, 223−229.
(52) Santoro, S. W.; Joyce, G. F. *Proc. Natl. Acad. Sci. USA* **1997**, *94*, 4262−4266.
(53) Li, J.; Lu, Y. *J. Am. Chem. Soc.* **2000**, *122*, 10466−10467.
(54) Wu, P. W.; Hwang, K.; Lan, T.; Lu, Y. *J. Am. Chem. Soc.* **2013**, *135*, 5254−5257.
(55) Mirkin, C. A.; Letsinger, R. L.; Mucic, R. C.; Storhoff, J. J. *Nature* **1996**, *382*, 607−609.
(56) Elghanian, R.; Storhoff, J. J.; Mucic, R. C.; Letsinger, R. L.; Mirkin, C. A. *Science* **1997**, *277*, 1078−1081.
(57) Park, S. J.; Taton, T. A.; Mirkin, C. A. *Science* **2002**, *295*, 1503−1506.
(58) Dubertret, B.; Calame, M.; Libchaber, A. J. *Nat. Biotechnol.* **2001**, *19*, 365−370.
(59) Rosi, N. L.; Giljohann, D. A.; Thaxton, C. S.; Lytton-Jean, A. K. R.; Han, M. S.; Mirkin, C. A. *Science* **2006**, *312*, 1027−1030.
(60) Seferos, D. S.; Giljohann, D. A.; Hill, H. D.; Prigodich, A. E.; Mirkin, C. A. *J. Am. Chem. Soc.* **2007**, *129*, 15477−15479.
(61) Seferos, D. S.; Prigodich, A. E.; Giljohann, D. A.; Patel, P. C.; Mirkin, C. A. *Nano Lett.* **2009**, *9*, 308−311.
(62) Zheng, D.; Seferos, D. S.; Giljohann, D. A.; Patel, P. C.; Mirkin, C. A. *Nano Lett.* **2009**, *9*, 3258−3261.
(63) Grabar, K. C.; Freeman, R. G.; Hommer, M. B.; Natan, M. J. *Anal. Chem.* **1995**, *67*, 735−743.
(64) Zhao, X.; Servos, M. R.; Liu, J. W. *J. Am. Chem. Soc.* **2012**, *134*, 7266−7269.
(65) Demers, L. M.; Mirkin, C. A.; Mucic, R. C.; Reynolds, R. A., III; Letsinger, R. L.; Elghanian, R.; Viswanadham, G. *Anal. Chem.* **2000**, *72*, 5535−5541.
(66) Chithrani, B. D.; G, A. A.; Chan, W. C. W. *Nano Lett.* **2006**, *6*, 662−668.
(67) Freese, C.; G, M. I.; Klok, H. A.; Unger, R. E.; Kirkpatrick, C. J. *Biomacromolecules* **2012**, *13*, 1533−1543.
(68) Alivisatos, A. P.; Johnsson, K. P.; Peng, X.; Wilson, T. E.; Loweth, C. J.; Bruchez, M. P.; Schultz, P. G. *Nature* **1996**, *382*, 609−611.
(69) Pan, W.; Zhang, T.; Yang, H.; Diao, W.; Li, N.; Tang, B. *Anal. Chem.* **2013**, *85*, 10581−10588.
(70) Li, N.; Chang, C.; Pan, W.; Tang, B. *Angew. Chem., Int. Ed.* **2012**, *51*, 7426−7430.
(71) Yun, C. S.; Javier, A.; Jennings, T.; Fisher, M.; Hira, S.; Peterson, S.; Hopkins, B.; Reich, N. O.; Strouse, G. F. *J. Am. Chem. Soc.* **2005**, *127*, 3115−3119.
(72) Zhang, Z.; Balogh, D.; Wang, F.; Willner, I. *J. Am. Chem. Soc.* **2013**, *135*, 1934−1940.
(73) Patel, P. C.; Giljohann, D. A.; Daniel, W. L.; Zheng, D.; Prigodich, A. E.; Mirkin, C. A. *Bioconjugate Chem.* **2010**, *21*, 2250−2256.

DOI: 10.1021/acs.analchem.5b00204
Anal. Chem. 2015, 87, 4829−4835